ICW note 1831

december 1987

PRELIMINARY RESULTS OF FIRST FIELD EXPERIMENTS IN THE QUATTARA DEPRESSION, WESTERN DESERT OF EGYPT

ing. W.G.M. Bastiaanssen and dr. M. Menenti

1. INTRODUCTION

The Institute for Land and Water Management Research (ICW) and the Research Institute for Groundwater (RIGW) of Egypt are carrying out an investigation into the hydrology of the depressions of the Western Desert of Egypt. The goal of these investigations is to estimate the total evaporation losses of groundwater in the depressions. The estimation procedures make use of satellite measurements of surface reflectance and surface radiation temperature.
The Quattara is the largest depression in the Sahara and is characterized by large portions where the groundwater table is present at shallow depths (e.g. 40 cm). Field work, therefore, has been focussed on this area.
The first field data collection campaign has taken place from 25 July through 10 August 1986. Figures, mentioned in the present report are based on this field campaign. The objectives of the field work were:

- to collect data directly required as ground-truth for the satellite measurements;
- to collect soil samples for further analyses in the laboratory;
- to gather impressions regarding the variability of types of salt crusts.

In figure 1, an overview is presented of the fieldwork in the Quattara depression. The radiometric measurements along the transect from the Mediterranean coast to the Quattara depression have been done to study the gradual transition in atmospheric radiative properties. This is required to correct the satellite measurements.
In table 1 and 2, a general overview of sites, variables measured and number of measurements is presented.

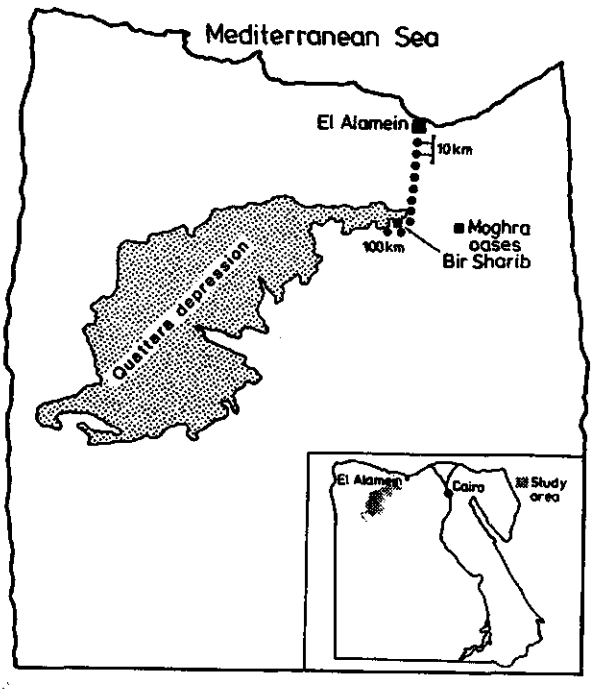

Fig. 1. Location map

Table 1: Data collection programme (surface energy balance)

Date	Site	Surface radiation temperature	Reflected shortwave irradiance	Shortwave irradiance	Spectro radiometer
29-7	Transect	-	-	-	6
30-7	Transect	-	-	-	4
31-7	Bir Sharib	2	-	-	1
1-8	Bir Sharib	6	5	5	4
2-8	Bir Sharib	1	-	-	-
3-8	Bir Sharib	3	2	2	2
4-8	Moghra oasis	5	5	5	3
5-8	Moghra oasis	12	6	6	6

Table 2: Overview of soil hydrological data collection

Site	Number of layers	Soil bulk density	Grain size distribution	K(h)	h(θ)	z(θ)	Ec	Cat	An
Sharib A	3	*	*	*	*	*	*	-	-
Sharib B	3	*	*	*	*	*	*	-	-
Sharib C	3	-	*	*	*	*	*	-	-
Moghra D/E	1	-	-	*	*	-	*	*	*
Moghra F	3	*	*	*	*	*	*	-	-

2. FIELD AND LABORATORY EXPERIMENTS

2.1. General

The actual evaporation flux can be estimated by applying satellite measurements of surface radiation temperature and shortwave surface reflectance into a linear combination function of surface energy balance and transport equation (MENENTI, 1984). This flux can be compared with the simulated vertical soil water flow through the unsaturated zone by means of models. Such models (e.g. SWATRE) give reliable estimates of fluxes if the soil hydrological properties and meteorological conditions are accurately known.

During field experiments, terms of the energy balance were measured, a new type of gauges to record automatically the groundwatertable was tested and samples for the determination of the soil hydrolological properties were collected.

A well known general feature of playa soils is the close relationship between the type of surface crusts and the depth of the watertable. The higher the watertable, the higher the amount of evaporation which results in more salt precipitation at surface level so that abundant salt aggregates with dominant white tones can be formed. In sequence of a higher salinity, the following types of surface crusts can be distinghuished:

- sand;
- sandcrust;
- hummocky;
- brown puffy;
- white puffy;
- salt cristal polygons.

2.1.1. Field experiments

The following terms of the surface energy balance were recorded:

Table 3a. Local time of the thermal infrared radiation temperature measurements

Date	Site	Measurement number							
		1	2	3	4	5	6	7	8
31-7	Bir Sharib	14.00	15.45	-	-	-	-	-	-
1-8	Bir Sharib	9.30	10.30	11.40	12.45	15.30	17.35	-	-
2-8	Bir Sharib	11.45	-	-	-	-	-	-	-
3-8	Bir Sharib	9.00	10.20	11.13	-	-	-	-	-
4-8	Moghra oasis	12.15	14.45	17.15	18.10	21.05	-	-	-
5-8	Moghra oasis	6.30	6.55	7.45	9.02	10.04	11.23	12.22	13.20
		14.57	15.44	17.02	18.08	-	-	-	-

Table 3b. Surface types of the thermal infrared radiation temperature measurements

Date	Site	Cork	Alagy	Dry sand	Brown puffy	White puffy	Hum mocky	Acacia	White saltcr	Reed
31-7	Bir Sharib	*	*	*	*	-	*	*	-	-
1-8	Bir Sharib	*	*	-	*	-	*	*	-	-
2-8	Bir Sharib	*	*	*	*	-	-	*	-	-
3-8	Bir Sharib	*	*	-	*	-	*	*	*	-
4-8	Moghra oasis	*	*	*	*	*	*	*	*	-
5-8	Moghra oasis	*	*	*	*	*	*	*	*	*

Note: The instrument was a Heimann KT-17 thermal infrared radiometer

Table 4. Incoming and reflected shortwave radiation

Date	Site	Surface type	Time			
			1	2	3	4
1-8	Bir Sharib	Sand with alagy	10.04	12.41	13.30	15.53
3-8	Bir Sharib	Brown puffy with alagy	8.42	10.06	-	-
4-8	Moghra oasis	Sandcrust with alagy	12.05	13.52	14.58	16.50
			17.40	-	-	-
5-8	Moghra oasis	White puffy	10.58	11.49	12.48	14.50
			16.04	16.50	-	-

Note: The instruments were 2 Kipp CM 2 pyranometers.

The hemispherical reflectance of the surface types listed in table 4 has been measured by means of two pyranometers, one upwards looking to measure the incident radiance and one downwards looking to measure reflected radiance.
An integration period of four minutes has been applied, while the calibration constant of pyranometers and integrators are given in table 5.

Table 5. Calibration coefficients of radiometers, 4 July 1986

	Pyranometer		Integrator	
Type	Kipp CM 2	Kipp CM 2	Kipp CC 2	Kipp CC 2
Serial no.	1350	1318	-	-
Calibration	$12.28*10^{-6}$	$9.83*10^{-6}$	10	10
Units	V $(W.m^{-2})^{-1}$	V $(W.m^{-2})^{-1}$	counts $(J.cm^{-2})^{-1}$	

Table 6. Spectral measurements of diffuse and direct solar radiation by means of a rotating band spectroradiometer (Guzzimeter), type Seli SRM 109

Date	Time	Site	Latitude
29-7	14.15	10 km Crossection	30.55
"	14.54	20 km Crossection	30.50
"	15.37	30 km Crossection	30.44
"	16.06	40 km Crossection	30.39
"	16.38	50 km Crossection	30.33
"	17.28	60 km Crossection	30.27
30-7	10.08	70 km Crossection	30.22
"	10.58	80 km Crossection	30.17
"	11.48	98 km Crossection	30.15
"	15.55	Bir Sharib	30.16
31-7	13.29	Bir Sharib	30.17
1-8	8.29	Bir Sharib	30.18
"	10.33	Bir Sharib	30.18
"	15.34	Bir Sharib	30.18
"	15.39	Bir Sharib	30.18
3-8	8.36	West of Bir Sharib	30.17
"	9.44	West of Bir Sharib	30.17
4-8	11.51	Moghra oasis	30.15
"	12.51	Moghra oasis	30.15
"	14.27	Moghra oasis	30.15
5-8	8.39	Moghra oasis	30.15
"	9.29	Moghra oasis	30.15
"	16.33	Moghra oasis	30.15
"	16.57	Moghra oasis	30.15
"	17.19	Moghra oasis	30.15
"	17.46	Moghra oasis	30.15

Two automatic waterlevel recorders have been installed in the Bir Sharib area, to measure the variation of the groundwater table and the direction of flow. Hourly values are stored on a removable memory (Eprom).

2.1.2. Laboratory experiments

The following table deals with the collected soil samples, which were analysed at the soil physical laboratory of the ICW at Wageningen.

Table 7a. Samples to obtain soil hydrological properties

Date	Profile number	Type of surface	Site	Phreatic level (cm)	Number of depths		
					K(h)	h(θ)	(z)
30-7	A	Sandcrust	Bir Sharib	95	3	3	7
1-8	B	Sand	Bir Sharib	100	3	3	9
2-8	C	Sand	Bir Sharib	65	3	3	6
4-8	D/E	White puffy	Moghra oasis	30	1	1	-
5-8	F	Brown puffy	Moghra oasis	70	3	3	6

Table 7b: Samples to obtain soil bulk properties

Profile number	Grain size distribut.	Soil bulk density	EC-2.5 unsat.	EC-2.5 sat.	Cat.	An.
A	3	3	-	3	-	-
B	3	3	-	3	-	-
C	3	3	-	3	-	-
D/E	-	-	3	-	1	1
F	3	3	-	3	-	-

2.2. Surface energy balance

2.2.1. Surface temperature

The surface radiation temperature of a number of surface types (see table 3b) has been measured by means of an infrared radiation thermometer (type Heimann KT 17). This instrument has been calibrated against a simple black body radiator. The result is shown in fig. 2. A

simple lineair relationship has been obtained between the corrected surface temperature T_0 and the measured surface radiation temperature T_0'.

$$T_0 = 0.88\ T_0' + 4.1 \qquad \text{(degree Celsius)} \qquad (1)$$

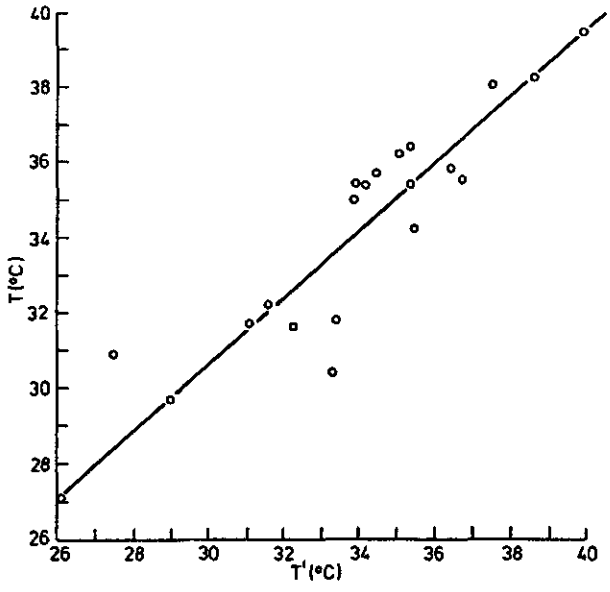

Fig. 2. Calibration data of thermal infrared radiometer; T_0', radiation temperature by means of thermal infrared radiometer; T_0, actual temperature of reference black body

In figure 3, the temperature of a few surface types present in the Moghra depression have been plotted. A cork panel has been taken as a reference. This panel is 6 cm thick and its thermal admittance is sufficiently low in comparison with the underlying soil to mask completely the effect of the latter on the surface temperature (see MENENTI, 1984).

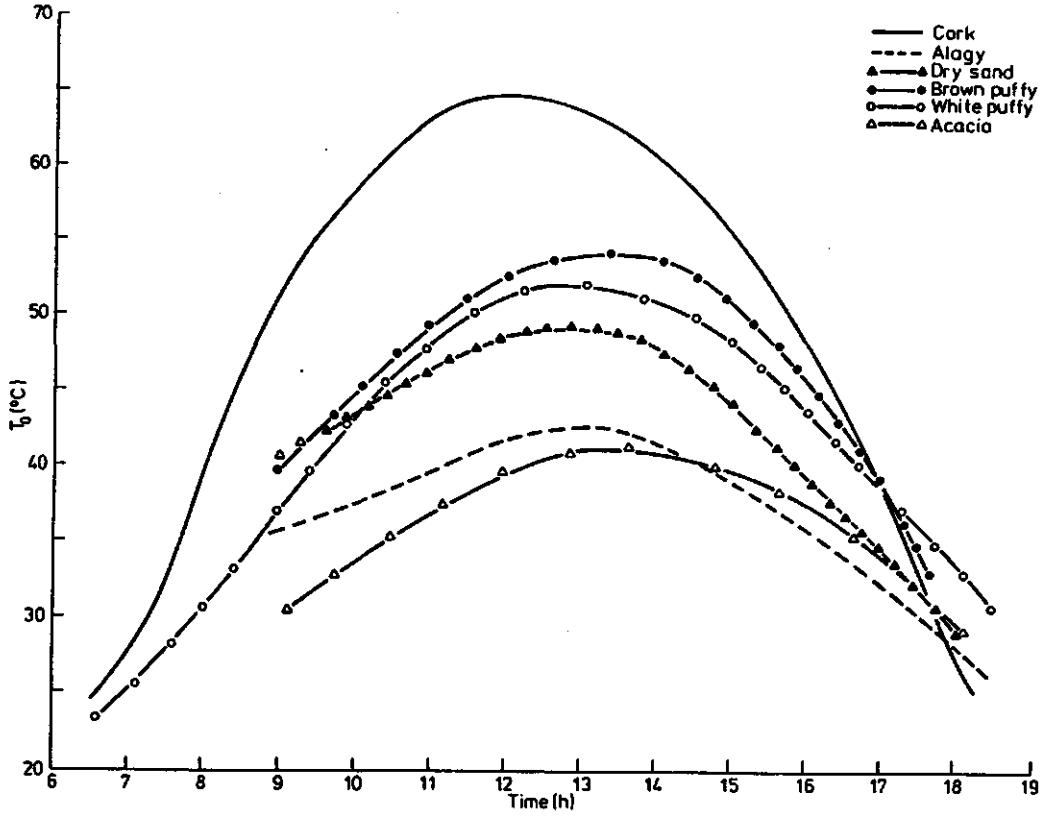

Fig. 3. Surface temperature measurements

It is worthwhile to spend a few comments on this figure 3. Experience gathered during the field work, has shown that this cork panel is a reliable criterion to compare radiation field conditions on different days. It quite clearly appears that, as designed, the cork has a negligible heat capacity, since the phase lag between its surface temperature and net radiation is essentially zero.

There is also a clear correlation between the phase lag and the surface type. The phase lag between the surface temperature of a particular surface and the net radiation above it, depends on the evolution of all terms of the surface energy balance and their relative weight (see VAN WIJK, 1963). This behaviour of playa soils will be further studied when results of the next field trips will become available.

The data in figure 3 show quite clearly the effect of salt encrustations on surface temperature. It is worth mentioning that the maximum surface temperature of sand is less than of both brown and white puffy crusts, which are clearly moister than sand. This result confirms once more the findings of previous work in Lybia (MENENTI, 1984). One reason for this seemingly strange thermal behaviour is the layered structure of playa soils, which structure gives lower thermal admittance values than sand. The effect of differences in surface reflectance must also be taken into account. The surface reflectance, at a sun zenith angle of zero degree, of the white puffy crust is 27% versus the 20% of the brown puffy. With a total irradiation of 1050 $W.m^{-2}$ around noon, this $\partial\alpha_0' = 0.07$ implies that net radiation (Rn) above the white puffy will be 74 $W.m^{-2}$ lower than Rn above brown puffy.
If everything else is being constant besides T_0, this Rn = 74 $W.m^{-2}$ implies a $\partial T_0 = -6$ K, which happens to be larger than the observed difference, $\partial T_0 = -4$ K. So the difference in reflectance alone may well explain the difference in T_0 between the brown and the white puffy crust. A similar reasoning can be applied to compare sand with the brown puffy: $\partial\alpha' = 0.12$, so Rn = -126 $W.m^{-2}$ and therefore $\partial T_0 =$ -11 K, which is again larger than the observed difference in T_0. To this respect it should be taken into account that the assumption of constant sensible heat (H) is not so realistic, since H will also decrease with a decreasing T_0, thus partially offsetting the impact of a higher α_0'.
The difference in maximum surface temperature between vegetation (Alagy and Acacia) and bare soil (see fig. 3) is also remarkable. Before explaining all of this difference as a difference in evaporation, the contribution of differences in surface reflectance and roughness must be estimated. One will consider firtst the effect of differences in aerodynamical resistance (r_a). The aerodynamical resistance of bare soil is relatively low around noon, because of thermal instabilities, say less than 100 $s.m^{-1}$. So the resulting increase in T_0 at constant latent heat and sensible heat flux, will be at most 2 K. The α_0' (ϕ s_u = 0) of this vegetation is 17%. By applying the preceding reasoning one obtain an upper bound estimate for the variation in T_0, namely $\partial T_0 = +6.5$ K. One can conclude therefore, that the observed difference $\partial T_0 = -15$ K between vegetation and bare soil is due to the higher evapotranspiration of plants.

2.2.2 Surface reflectance

The hemispherical reflectance has been obtained by dividing reflected by incident radiance. The so obtained albedo, is surface crust dependant (see table 8).

Table 8. Surface reflectance for different crust types at $\phi_{su} = 0$

Surface type	Surface reflectance
Coarse sand	32%
Brown puffy	20%
White puffy	27%
Sand crust	11%

The surface reflectance of hypersaline soils changes considerably during the day (MENENTI, 1984), partly because of the daily drying-wetting cycle of the soil surface and partly because of the sun zenith angle dependance. In figure 4, surface reflectance (α_0) measurements, collected over sand at Bir Sharib, have been plotted together with α_0-values calculated by means of inversion of equation (2) given by BARTMAN (1980) relating α_o to the sun zenith angle (ϕ_{su}):

$$\alpha_0 = \alpha_0' \; 2.444 \; [1-\cos \phi_{su} \; \ln(1+1/\cos \phi_{su})] \qquad (-) \qquad (2)$$

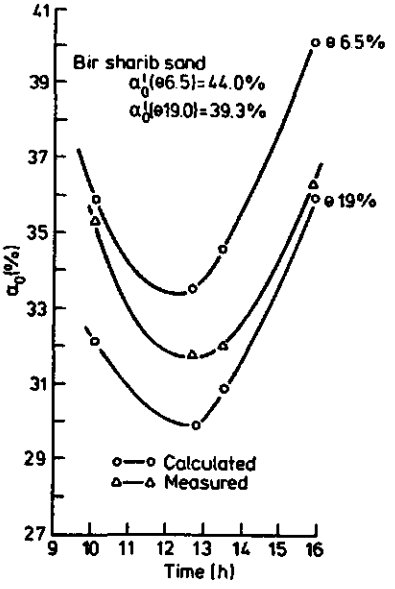

Fig. 4. Surface reflectance measurements

It clearly appears that the equation reproduces satisfactorily the daily variation of surface reflectance, due to ϕ_{su} only. The results did not show the expected daytime drying of the soil surface (see figure 4, $\theta_{(morning)} = 0.19\ cm^3.cm^{-3}$, $\theta_{(evening)} = 0.065\ cm^3.cm^{-3}$). Since the α_0'-values ($\phi_{su} = 0$) represent a kind of mean daily value regarding moisture content of the $\alpha_0(\theta)$ function fitting each individual measurement, the daytime drying of the soil surface implies an increasing trend in the α_0 values. During the day, however, the percentage of diffuse radiation (R_{swdf}) does also increase. This can expressed with the equation given by MAKAROVA et al. (1973):

$$\alpha_0 = \alpha_0' \left[1+2.5\left(1.25 - \frac{R_{swdf}}{R_{sw}}\right)(1 - \alpha_0')\sin\frac{3}{2}\right] \phi_{su} \ (-) \qquad (3)$$

This equation shows that the two effects on α_0 tend to compensate each other:

- drying of the soil surface gives higher α_0-values;
- increase of the ratio R_{swdf}/R_{sw} gives lower α_0-values.

The latter effect will be assessed in the next paragraph by means of spectral measurements of total and diffuse irradiance.

2.2.3. Atmospheric correction

Satellite images should be corrected for the influence of atmosphere. This can be done with ground based measurements on atmospheric conditions. Clouds, watervapour and aerosols will in principle affects the amount of scattering and absorption. If one is able to divide the total irradiance into diffuse and direct radiance for different bands of the spectrum, an estimation of the optical thickness of the atmosphere and the size distribution of aerosols can be obtained.
An experimental type of rotating band spectroradiometer has been developed by Guzzi, which apparatus measures the spectral quality of the direct and diffuse solar radiation in 9 wavelength intervals for a total spectral range between 0.395-1.055 μm (table 9). The scanning speed for each band is 10 samples per second.

Table 9. Characteristics of Guzzi spectroradiometer

Bandnumber	Bandwith (μm)
1	0.395 - 0.405
2	0.435 - 0.445
3	0.495 - 0.505
4	0.515 - 0.525
5	0.545 - 0.555
6	0.675 - 0.685
7	0.735 - 0.745
8	0.925 - 0.935
9	1.045 - 1.055

An estimation of the effect of scattering can be quickly obtained by plotting the measurements in bands 1,5 and 9. An example can be found in figure 5. The units on the vertical axis are arbitrary. As can be seen from such graphs, the time required for a single measurement is

50 seconds. During this time, the rotating band covers twice the sensor on top of the meter so that only the diffuse part of the total irradiance can be measured. This feature can be found back as the two minimum values on the graph.

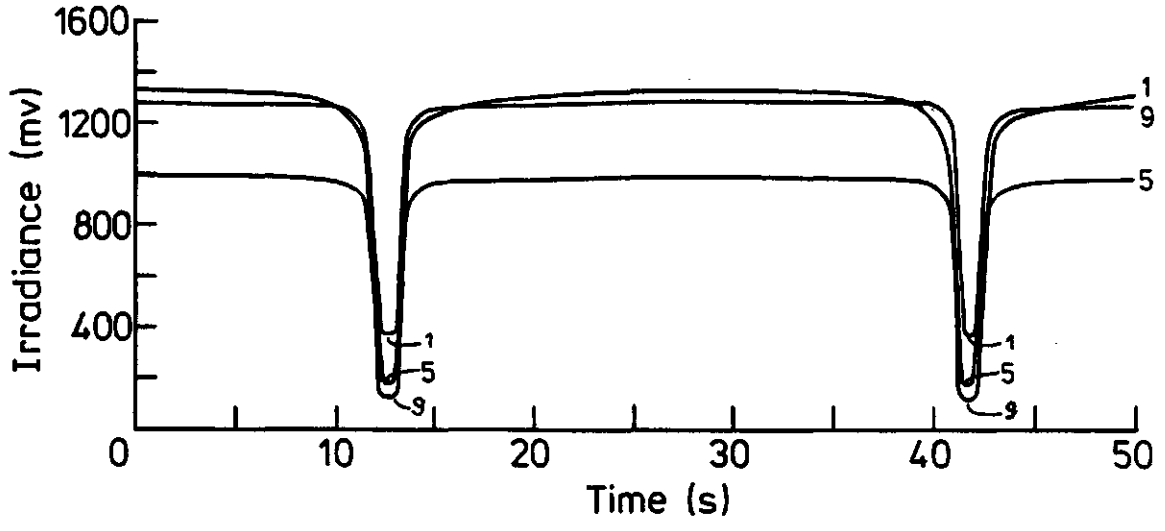

Fig. 5. Single experiment with Guzzi spectroradiometer

The average amount of scattering over the three different bands has been summarized for a weekly period in table 10. In general it can be concluded, that band 1 shows larger scattering effects, due to Raleigh scattering of water molecules. A graph of single datapoints can be found in figure 6.

Table 10. Ratio of diffuse to total irradiance

Bandnumber	Diffuse/total irradiance (%)
1	40.3
5	18.0
9	13.8

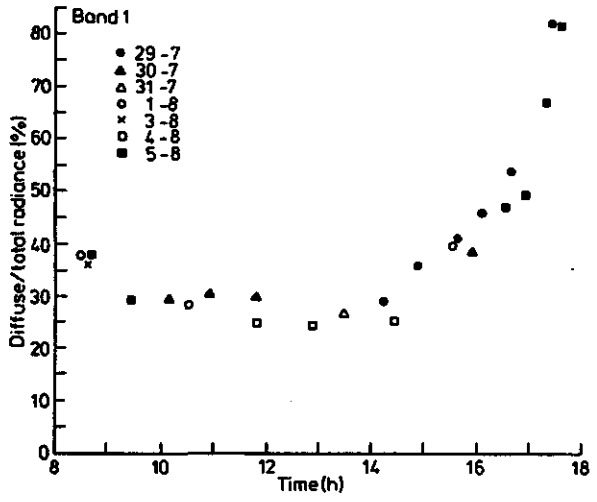

Fig. 6. Ratio of diffuse to total irradiance

At lower solar altitudes, the percentage of diffuse radiation is larger then at higher solar altitudes. Hence, equation (3) in paragraph 2.2.2. will provide lower α_0-values during the afternoon. So, it is very well possible that a daytime drying and scattering cycle, affect the reflectance simultaneously.

2.2.4. Example of estimation of net radiation for different surface types

To obtain net radiation values applying to different surface types, the following procedure has been applied; at a field plot net radiation (Rn), reflected radiation ($\alpha_0 R_{sw}$) and surface radiation temperature (T_0) are measured. Solar radiation (R_{sw}) is measured at a central site:

i = 1, ...n (sites);
at i = 1: solar radiation
at i = 2: net radiation, reflected radiation and surface radiation temperature (air temperature optional).
at i = 3, ...n reflected radiation and surface radiation temperature.

The radiation balance equation at site 2 can be written as:

$$Rn_{,2} = R_{sw,i} - \alpha_{0,2} R_{sw,2} + L_{a,i} - L_{s,2} \quad (4)$$

where L_a is the longwave radiation emitted by the atmosphere and L_s the longwave radiation emitted by the soil surface. Introducing $R_{sw,i} = R_{sw}$ and $L_{a,i} = L_a$,the latter can be expressed as follows:

$$L_a = Rn_{,2} + \alpha_0 R_{sw,2} - R_{sw} + \sigma T_{0,2}^4 \quad (5)$$

where $T_{0,2}$ is the surface radiation temperature at site 2 and σ the Stefan Boltzmann constant. If required, either the apparent sky radiation temperature (T_{sky}), or the apparent emissivity of the atmosphere (ϵ') can be obtained:

$$T_{sky} = \left(\frac{L_a}{c}\right)^{1/4} \quad (K) \quad (6)$$

$$\epsilon' = \frac{L_a}{\sigma . T_a^4} \quad (-) \quad (7)$$

where T_a is the air temperature at some reference height. The so obtained values for ϵ' are ϵ'(day) = 0.89 and ϵ'(night) = 0.75. Then net radiation values at each plot where α_0 and T_0 are measured can be calculated as follows:

$$Rn_{,i} = R_{sw} - \alpha_{0,i} R_{sw} + L_a - c T_{0,i}^4 \quad (8)$$

The ϵ' values can be applied to assess the accuracy of semi-empirical relationships (e.g. DOORENBOS and PRUITT, 1977) with the vapour pressure.

$$\epsilon' = 0.66 + 0.044 \sqrt{E_a} \quad (9)$$

where E_a (mbar) is the actual vapour pressure. New values of the coefficients in eq. (9) can eventually be derived.
The just outlined procedure can be applied in much the same way to map net radiation with satellite measurements ($\alpha_{0,i}$, $T_{0,i}$). Furthermore the ratio of net radiation to solar irradiation is a usefull characteristic of the energy balance of different surface types. In figure 7 the results applying to bare coarse sand and brown puffy are shown. The ratio Rn/Rsw appears rather constant with the surface.

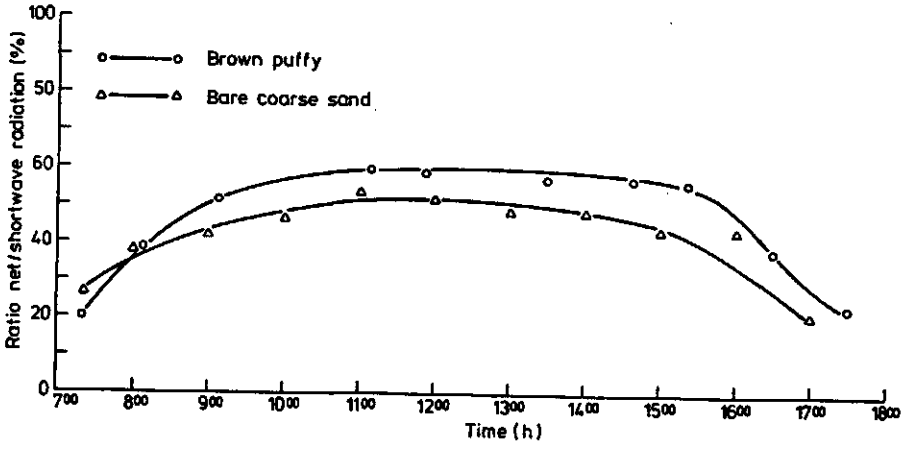

Fig. 7. Ratio of net to solar irradiation

2.3. Soil hydrological properties

2.3.1. General

Calculation of capillary rise is in principle a reliable method to calculate the mean evaporation rate in playas. By taking samples close to the shallow watertable, one has a good opportunity to avoid the difficulties involved in the determination of soil hydrological properties in the dry range, i.e. at rather small θ values and rather large salt content.
This potential advantage is offset by the hypersaline nature of playa soils. At these extremely high concentrations, salt minerals affect soil characteristics in many ways:

- soil bulk density is much smaller (and porevolume larger) than usual;
- grain size distribution is smoothed out by the presence of salt crystals and aggregates;
- physical properties of soil water are deeply modified by the presence of dissolved salts in extremely high concentrations;
- soil hydrological properties, i.e. $h(\theta)$ and $K(h)$ relationships, are deeply modified, partly because of changes in physical properties of soil water.

The problems are compounded by the usual laboratory techniques for the determination of soil properties. These techniques typically involve wetting or saturating soil samples. So the total salt content and, possibly, salt concentration in the soil sample are modified by the experimental approach, thus affecting the properties one wishes to measure. Some of these modifications can be corrected for, if the original salt concentration in the sample can be estimated. In the following chapter, examples will be presented to illustrate how these corrections can be calculated.

2.3.2. Determination of soil composition

As has been pointed out before, playa soils contain water of a high level of salinity. The type of surface crust is strongly related with the level of the groundwatertable. Chemical analyses have only been performed for a white puffy type of crust situated at Moghra oasis. The electric conductivity has been determined for a 1/2.5 soilpast extract (EC-2.5) (table 11).

Table 11. Electrical conductivity of a 1/2.5 soilpast; Moghra depression

Depth (cm)	EC-2.5 ($mS.cm^{-1}$)
2	44.8
5	41.3
10	40.4

Note: Temperature 19 degree Celsius

It could be seen that the degree of salt precipitation at surface level is larger than inside the topsoil. Specie analyses were required to determine the type of salt crystals and dissolved species. The shaking period of the soil past extract (1/2.5) was one hour. The assumption is made that the mixture contains enough water to dissolve all the species of the solid part. The result of the specie analyses are presented in table 12.
The actual soil water content plays an important role because changes of the soil water content affect the equilibrium condition of the species until the new equilibrium condition is reached.

Table 12. Dissolved ions in the liquid fase of a 1:2.5 soil paste; white puffy crust

	CATIONS			ANIONS		
	Absolute		Rela-	Absolute		Rela-
	meq/100 gr soil	mass % of soil	tive %	meq/100 gr soil	mass % of soil	tive %
Na	145.9	3.4	74.8	-	-	-
K	1.7	0.1	0.9	-	-	-
Ca	9.1	0.4	9.3	-	-	-
Mg	14.6	0.4	15.1	-	-	-
Cl	-	-	-	164.6	5.8	60.5
SO_4	-	-	-	13.0	0.6	4.8
CO_3	-	-	-	94.5	2.8	34.7
			100.1			100.0

It can be easily seen that this type of soil is a typical halite one. Aggregates of Calciumcarbonate are probably present. The Exchangeable Sodium Percentage (ESP-value) can be read as 74.8 percent. The problem involved is the actual equilibrium concentration between the dissolved species and the oversaturated complexes. The amount of really dissolved species have to be applied on the correction of the unsaturated hydraulic conductivity and water retention curve as analysed under laboratory conditions.

2.3.3. Effects of soil composition on soil structure

The high salinity of playas affects the vertical flow towards the surface:

- a gradient of salinity inside the topsoil will cause an additional osmotic pressure head;
- the dissolved species in the soil moisture change the bulk properties of liquid water (see also paragraph 3.1.);
- the salt cristals change the natural structure of the soil.

Large salt cristals and polygones change the texture of the soil considerably. This can be studied by means of sieve shaking equipment to obtain the grain size distribution (table 13).

Table 13. Grain size distribution of various samples

Sample	M_{50} µm	38 µm	38-53 µm	53-150 µm	150-300 µm	300-425 µm	425-600 µm	600-2000 µm	>2000 µm
A1	376	0.1	3.1	8.7	26.2	19.7	17.2	24.8	0.3
A2	343	0.1	1.2	8.6	30.9	26.9	18.1	14.0	0.1
A3	243	0.1	1.6	11.7	59.1	11.9	6.6	7.1	1.9
B1	393	0.1	3.5	9.5	23.7	17.8	15.8	29.5	0.1
B2	377	0.1	1.3	8.1	26.7	22.4	20.0	21.3	0.1
B3	453	0.1	0.7	7.3	22.0	17.1	17.8	34.1	0.1
C1	284	0.3	1.1	16.0	36.5	15.3	12.2	18.4	0.1
C2	498	0.0	0.5	8.7	20.9	12.8	17.0	39.9	0.0
C3	274	0.0	2.5	18.3	35.3	15.1	13.1	14.9	0.0
F1	219	0.2	7.3	18.3	52.0	5.0	3.9	7.0	6.4
F2	407	0.0	4.2	15.9	17.8	14.1	16.9	29.1	2.0
F3	175	0.9	16.6	31.2	16.4	7.8	7.7	14.1	5.2

In general it can be concluded that playas consist of a coarse sandy type of soil. The overall Median 50 figure (M_{50}) is about 360 µm. It seems that the white puffy (profile F) has a lower median (M_{50} = 270 µm) which can be related to the presence of salt cristals. The salt minerals possess the particle sizes of loam, and gives the bottom therefore a finer structure. This feature can be detected either by studying the soil water retension characteristic such as in paragraph 2.3.4., or by the tendency of the higher the salinity, the lower the M_{50} figure. The salinity is expressed as the electric conductivity of a 1/2.5 soil extract after saturation. This practice has to be done because grain size distribution and bulk density were both obtained after saturation as well. Their mutually relationship appears from table 14.

Table 14. Relation of soil compostion with bulk properties

Profile	Depth (cm)	Groundwater level (cm)	M_{50} (μm)	EC-2.5 $mS.cm^{-1}$ saturat.	Bulk density $kg.m^{-3}$
A1	5	95	376	6.7	1180
A2	38	95	343	3.5	1610
A3	67	95	243	3.4	1800
B1	1	100	393	4.0	1710
B2	31	100	377	3.0	1630
B3	90	100	453	2.4	1830
C1	1	65	284	4.7	-
C2	15	65	498	0.4	-
C3	55	65	274	1.1	-
F1	0	70	219	13.4	1050
F2	30	70	407	7.1	980
F3	60	70	175	13.9	920

It becomes clear that the structure near the groundwatertable is quite normal for profiles in arid regions (ρ_b = 1.8 $gr.cm^{-3}$, EC-2.5 = 3.0 $mS.cm^{-1}$). However the hypersaline topsoil (ρ_b = 1.3 $gr.cm^{-3}$, EC-2.5 = 8 $mS.cm^{-1}$) is typical of playas and indicates the presence of evaporation.

The extremely low density values of the topsoil (e.g. sample F1, F2 and F3) are a result of water saturating the samples in the laboratory. Soluble salts are leached out in large quantities immediately. This is a process of great interest, because the same reaction shall occur during natural recharge.

2.3.4. Determination of soil hydrological properties

The soil moisture pressure head (h total) can be written as:

$$h_{total} = h_{matric} + h_{osmotic} \quad (m) \qquad (10)$$

At low salinity, osmotic potential is neglected. This assumption does not apply to playa soils. To simulate soil water flow in the unsaturated zone, the relationship between soil moisture pressure head (h) and soil water content (waterretension curve) and between unsaturated capillary conductivity and soil moisture pressure head (K(h)) are needed.

The K(h) and h(θ) relationships in the low h range, i.e. $|h|>-800$ cm have been obtained at the soil physical laboratory of ICW by means of an instrument with tensiometers, described by BOELS et al (1978). The h(θ) values PF = 3.4 and PF = 4.2 have been obtained by means of a pressure membrane appartus. It appears that the h(θ) relationship of sample A3 (see fig. 8a) is a typical one for a coarse sand profile, while sample F3 (see fig. 8b)) bends to the behaviour of a fine textured soil. This is in full agreement with the preceeding comments on the effect of salt crystals on soil texture.

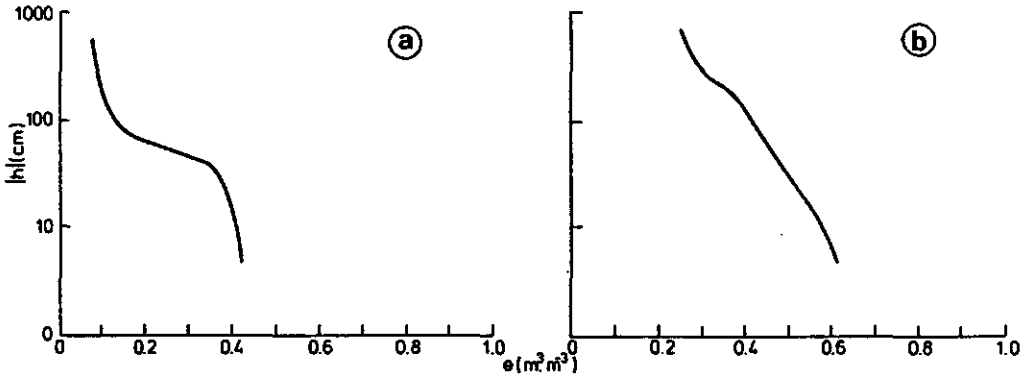

Fig. 8. Soil water retention curves

The influence of salts on osmotic potentials and texture is evident via the soil hydrological properties e.g. a white puffy type of soil contains a larger moisture content at the same pressure head as a standard sandy type of soil. This results in a wetter profile than sample A3, which is in correspondance with the derived moisture profile $z(\theta)$ (fig. 9).

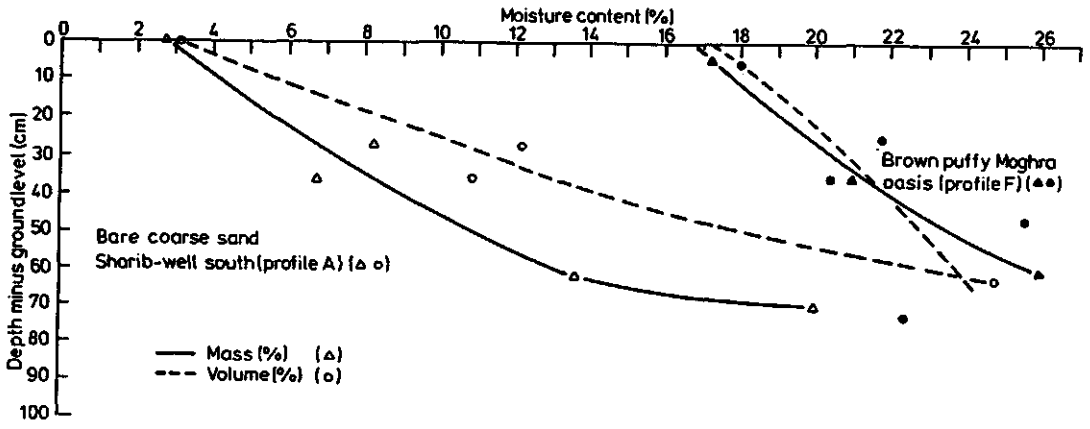

Fig. 9. Moisture versus depth profile

Consequently a larger percentage of water filled pores increases the unsaturated hydraulic conductivity (K(h)). Graphical expressions of the K(h) relationship are presented in figure 10.

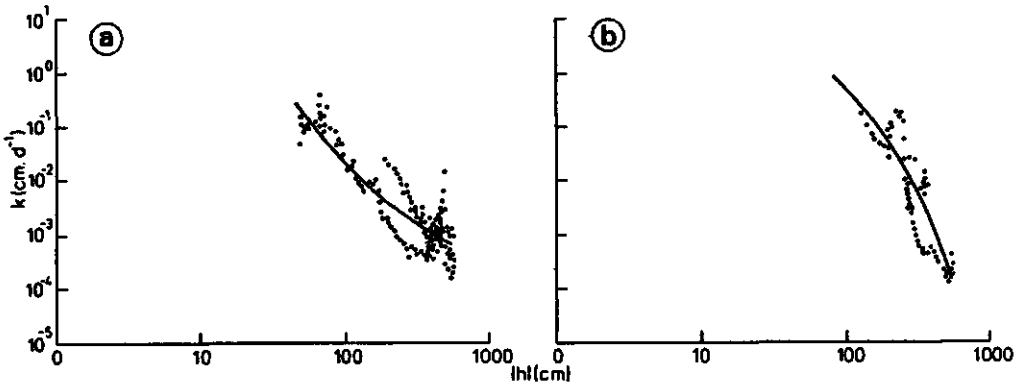

Fig. 10. Unsaturated hydraulic conductivities

2.3.5. Effects of soil hydrological properties on capillary rise

To study the effect of salt minerals on the upward flow, the program CAPSEV (J.G. Wesseling et al., 1984) has been applied. This program integrates numerically the steady state Darcy equation for unsaturated conditions. The result of the calculation for any particular flux-value is the distribution of pressure head with depth able to maintain that particular flux. When steady state conditions do actually occur in the field, a single measurement of h at some distance, say 15 cm above the water table, gives the value of actual evaporation with the help of tables, calculated as done with table 15.

Table 15: Maximally possible fluxes as obtained with program CAPSEV; a varying watertable between 10 and 150 cm below surface and corresponding pressure heads in a range from -20 until -1000 cm for profile A3 (coarse sand) has been considered.

MAXIMALLY POSSIBLE FLUXES (cm/day)

PROFILE BIR SHARIB A3

PR. HEAD (CM.)	*	GROUNDWATER LEVEL (CM. BELOW SURFACE) 10.	20.	30.	40.	50.	60.	70.	80.	90.	100.	110.	120.	130.	140.	150.
-20.	*	0.056	0.002	0.000	0.000	0.000	0.000	0.000	0.000	0.000	0.000	0.000	0.000	0.000	0.000	0.000
-40.	*	0.154	0.051	0.019	0.002	0.000	0.000	0.000	0.000	0.000	0.000	0.000	0.000	0.000	0.000	0.000
-60.	*	0.255	0.101	0.051	0.027	0.010	0.002	0.000	0.000	0.000	0.000	0.000	0.000	0.000	0.000	0.000
-80.	*	0.356	0.152	0.084	0.052	0.030	0.018	0.008	0.002	0.000	0.000	0.000	0.000	0.000	0.000	0.000
-100.	*	0.500	0.224	0.132	0.086	0.059	0.041	0.028	0.018	0.010	0.004	0.000	0.000	0.000	0.000	0.000
-150.	*	0.751	0.349	0.216	0.151	0.109	0.082	0.065	0.049	0.039	0.031	0.022	0.016	0.012	0.006	0.002
-200.	*	-1.000	0.474	0.301	0.212	0.159	0.126	0.099	0.080	0.066	0.055	0.046	0.037	0.030	0.024	0.021
-400.	*	-1.000	0.976	0.634	0.462	0.359	0.292	0.242	0.207	0.177	0.154	0.137	0.121	0.107	0.095	0.086
-550.	*	-1.000	-1.000	0.884	0.649	0.509	0.417	0.349	0.301	0.262	0.230	0.204	0.184	0.166	0.151	0.136
-1000.	*	-1.000	-1.000	-1.000	-1.000	-1.000	0.866	0.735	0.638	0.560	0.500	0.451	0.407	0.374	0.343	0.317

NOTE : The figure -1.000 indicates the occurrence of a flux > 1.0 cm/day !!

3. CORRECTING SOIL HYDROLOGICAL PROPERTIES FOR THE EFFECTS OF SALTS AND TEMPERATURE

3.1. Differences between field and laboratory soil solute concentration of samples

Halite cristals have the character of easily dissolving when water is applied. Preparing the samples for laboratory experiments, all the pores have to be saturated with water. During this saturation process, the electric conductivity of the drainage water has been measured at fixed intervals.

The total of 13 soil samples were divided over 2 different reservoirs. Consequence of this treatment is that only a mean leached quantity of salts for a single sample can be estimated. Assumed hereby is that all solutes derived from Sodiumchloride crystals.

The most saline samples were placed in the same reservoir, with water in the reservoir having a final electric conductivity of 36 $mS.cm^{-1}$ in 3.439 litre of drainage water (fig. 11). This is a total quantity of 1260 mmol, so that every sample (content 0.63 litre) lost 180 mmol NaCl in a weekly period! The latter figure for the second reservoir is 24 mmol NaCl per week. This weigth has to be added to the soil bulk density after saturation to obtain the density before the saturation process. The average open water evaporation inside the laboratory was 1.0 $mm.day^{-1}$.

The solute concentration in the samples at the beginning of the laboratory test can be estimated with the final equilibrium concentration of the drainage water (0.36 $mol.l^{-1}$). During the test, the solute concentrations will increase, because the soil water will evaporate.

The osmotic contribution to the total pressure head, can be derived from the salt concentration. The osmotic contribution will however not be determined by the ceramic cup technique used during the test i.e. the solute concentration inside the soil moisture and inside the tensiometer are equal. This implies that the pressure head measured by tensiometers shows no deviation with the suction caused by matric forces.

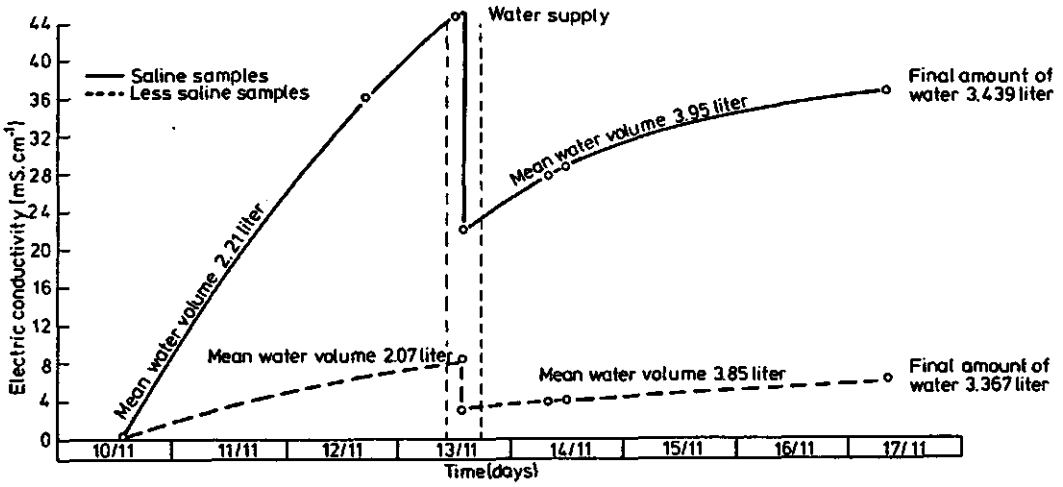

Fig. 11. Salt leaching during saturation process; laboratory experiment

Hence the measured pressure head has only to be corrected for the effect of salts and temperature on the bulk properties of water. The matric pressure head can be mathematically expressed as:

$$h_m = \frac{1}{\rho_w g} \left(\frac{2\,\sigma_{wa}}{R_m}\right) \quad (m) \qquad (11)$$

where: h_m = matric pressure head (m)
ρ_w = density of liquid water ($kg.m^{-3}$)
g = gravitational constant ($m.s^{-2}$)
σ_{wa} = surface tension of water against air ($N.m^{-1}$)
R_m = mean pore radius (m)

Surface tension and density are besides being salt concentration dependant, also temperature dependant. As indicated before, there is a large thermal amplitude during the daytime cycle at surface level, while the groundwater table has a rather constant temperature value (18 degree Celcius). In another words; thermal corrections have to be made.

3.2. Correcting the h(θ) relationship

The partial derivatives towards temperature (T) and salt concentration (x) of the matric pressure head become:

$$\frac{\delta h}{\delta T} = \frac{\rho_w \cdot h}{\sigma_{wa}} \frac{\delta}{\delta T} \left(\frac{\delta_{wa}}{\rho_w}\right) \qquad (12)$$

$$\frac{\delta h}{\delta x} = \frac{\rho_w \cdot h}{\sigma_{wa}} \frac{\delta}{\delta T} \left(\frac{\delta_{wa}}{\rho_w}\right) \qquad (13)$$

If for instance the solute concentration under field conditions is 6 $mol.l^{-1}$ and 2.5 $mol.l^{-1}$ in the drainage water, the deviation of the matric pressure head can be obtained as - 31 cm for the effect of salts only. The following figures are applied:

ρ_w (X=6.0 $mol.l^{-1}$) = 1.266 E3 $Kg.m^{-3}$

ρ_w (X=2.5 $mol.l^{-1}$) = 1.110 E3 $Kg.m^{-3}$

δ_{wa}(X=6.0 $mol.l^{-1}$) = 8.429 E2 $N.m^{-1}$

δ_{wa}(X=2.5 $mol.l^{-1}$) = 7.756 E2 $N.m^{-1}$

Temperature at laboratory 20 degree Celsius

Measured pressure head at laboratory -650 cm

The same procedure can be applied to account for the effect of temperature on pressure head.

3.3. Correcting the K(h) relationship

The unsaturated hydraulic conductivity can be explicitly related to the saturated conductivity by introducing a relative unsaturated capillary conductivity term (B(h)). Furthermore, the saturated conductivity can be split up:

$$K(h) = B(h) \cdot K_{sat} = B(h) \cdot \rho_w \cdot g \cdot \frac{K}{\eta_w} \qquad (m.s^{-1}) \qquad (14)$$

where: K = soil specific permeability (m^2)
η_w = viscosity of liquid water ($N.s.m^{-2}$)
g = gravitational constant ($m.s^{-2}$)
ρ_w = density of liquid water ($kg.m^{-3}$)
$B(h)$ = relative unsaturated conductivity (-)
K_{sat} = saturated conductivity ($m.s^{-1}$)

The soil specific permeability is the only soil particle dependant parameter while in fact the relative unsaturated conductivity is the only soil water content dependant variable.
The equations for the partial derivatives towards the salt and temperature concentration are:

$$\frac{\delta K(h)}{\delta T} = \frac{\rho_w\, g\, K}{\eta_w} \frac{\delta\, B(h)}{\delta h} \frac{\delta h}{\delta T} + g\, K\, B(h) \frac{\delta}{\delta T} \left(\frac{\rho_w}{\eta_w}\right) \qquad (15)$$

$$\frac{\delta K(h)}{\delta x} = \frac{\rho_w\, g\, K}{\eta_w} \frac{\delta\, B(h)}{\delta h} \frac{\delta h}{\delta x} + g\, K\, B(h) \frac{\delta}{\delta x} \left(\frac{\rho_w}{\eta_w}\right) \qquad (16)$$

The data of paragraph 3.2 is applied to correct on K(h). The salt related viscosity is 1.56E-04 $N.s.m^{-2}$ and 2.34E-04 $N.s.m^{-2}$ for laboratory and field conditions respectively. From the saturated conductivity (50 $cm.d^{-1}$), the soil specific permeability can be determined as being 8.375E-14 m^2. If a pressure head of 650 cm with K(h) being 0.60E-03 $cm.d^{-1}$ is assumed, the correction on K(h) for salinity will be - 0.12E-03 $cm.d^{-1}$. The same calculations can be done to correct for temperature differences.

4. IMPROVED EXPERIMENTAL APPROACH

As has been stressed in this note, corrections on the soil hydrological properties as obtained at the laboratory, have to be applied to account for differences with the field conditions.
Ceramic cups can only measure the matric pressure head. A method has to be developed to account for the effect of matric pressure head on the total pressure head. Then separate corrections for matric and osmotic forces can be applied.
Regarding the matric pressure head, analyses of soil water directly extracted in the unsaturated soil have to be done. These water samples can be collected with a ceramic cup (tensiometer) connected with a simplified apparatus to apply suction. During saturation at the laboratory, every sample should be placed in a single reservoir. Only then, reliable corrections can be applied.
Furthermore, a systematically description of the different types of crusts and profiles have to be made. Then it will be easier to link the soil composition with the bulk properties and consequently a better parameterization of the heterogeneous structure of a playa soil.
It could be an idea to measure the salt concentration before saturation by means of the soil past extract method (e.g. EC-20,EC-50). An impression about the total abundance of salts under field conditions and its variation can then be recorded.
More efforts have to be spent to study the diurnal variation of the surface reflectance. The relationship between reflectance, sun zenith angle, ratio diffuse to direct shortwave radiation and the surface wetness have to be mathematically expressed.

REFERENCES

BOELS, D., J.B.H.M. VAN GILS, G.J. VEERMAN and K.E. WIT, 1978. Theory and system of automatic determination of soil moisture characteristics and unsaturated hydraulic conductivities. Soil Science 126(4): 191 - 199.

FEDDES, R.A., P.J. KOWALIK and H. ZARADNY, 1978. Simulation of field water use and crop yield. Simulation monographs. 188 p.

FORSYTHE, W.E., 1969. Smithsonian physical tables. ninth revised edition, Smithsonian Institute, Washington DC. 827 p.

MENENTI, M., 1984. Physical aspects and determinations of evaporation in deserts applying remote sensing techniques. Report no. 10 (Special issue), 202 p.

UNITED STATES SALINITY LABORATORY STAFF. Diagnosis and Improvement of Saline and Alkali soils, Agricultural Handbook No. 60.

VEUGEN, L.M.M., H.T.C. VAN STOKKOM, 1985. An atmospheric correction method using Guzzi-spectroradiometer input data, ESA SP-247.

WEAST, R.C., Handbook of Chemistry and Physics, 48th edition, 1967-1968, The chemical Rubber Co.

WIJK, W.R., 1963. Physics of plant environment. John Wiley and Sons, Inc., New York.